Dynamic Correlation Study
Transfer Case Housings

William R. Kelley, L. Dean Isley, Thomas J. Foster
Borg-Warner Automotive - Powertrain Systems
Sterling Heights, MI, USA

Abstract

The process of casting design in the automotive industry has been significantly refined over the years through the capabilities of advanced computer aided design and engineering tools. One of the significant benefits of these computer aided capabilities is the direct access to CAD geometry data, from which finite element models can be quickly developed. Complex structures can be meshed and analyzed over a relatively short period of time. The application of advanced finite element analyses such as structural modification and optimization are often used to reduce component complexity, weight and subsequently cost. Because the level of model complexity can be high, the opportunity for error can also be high. For this reason, some form of model verification is needed before design decisions made in the FEA environment can implemented in production with high confidence. Dynamic correlation, comparison of mode shapes and natural frequencies, is a robust tool for evaluating the accuracy of a finite element model. This paper describes the application of dynamic correlation techniques for verification of mass and stiffness distribution in two complex FEA models of aluminum die cast housings.

1.0 Introduction

This paper describes a dynamic correlation study as performed on structural elements in an automotive powertrain; specifically, a transfer case assembly. A transfer case is the device which transfers torque to both front and rear wheels in four-wheel drive and all-wheel drive vehicles. It is mounted to the output of the transmission and is coupled to the front and rear axles through propeller shafts. The housings of the transfer case locate the internal shafts, provide structural rigidity and seal in lubricant. The transfer case used in this study has a two piece enclosure. The front half bolts directly to the rear of the transmission and is referred to as the "case". The front case is an elliptical bowl with a cylindrical projection on one side of its face, and a bore at the other side which supports the output shaft bearing. The rear half is referred to as the "cover" and is joined to the case with numerous bolts and sealant. The rear cover is basically a flat plate with a cylindrical projection at one end referred to as the extension. Both components are stiffened with ribbing and both are made from die cast SAE 318 Aluminum.

Because the transfer case housings perform a structural role, they must be designed to withstand input loads from the driveline, which can be quite significant, particularly in off-road driving conditions. At the same time, the cost of materials and the customers strict weight requirements dictate they be designed with a minimum amount of material. To achieve these ends, finite element techniques have been used extensively for some years.

The complex shape of the transfer case housings requires the finite element models which represent them to be rather intricate, consisting of a combination of different element types and a fairly high number of degrees of freedom. As the complexity of the model increases, so does the opportunity for error, which creates a need for some form of verification. In this study, dynamic correlation techniques are used to gauge the accuracy of the finite element representation of the housings. Treating each half of the transfer case enclosure independently, analytical and experimental models were developed, using Finite Element Analysis (FEA) and Experimental Modal Analysis (EMA) techniques. Experimental modal surveys were conducted, and the frequencies and mode shapes were compared to those extracted from the MSC/NASTRAN [1] models. Techniques such as the Modal Assurance Criteria (MAC) [2] were used to compare the vectors, and observations made about the potential for improvements. The difficulties encountered and the limitations and liabilities of the tools used are also discussed.

2.0 Theory

Each of the methods described above is briefly reviewed herein; more detailed theoretical development is contained in the references.

2.1 Finite Element Model

To obtain poles and frequencies from the finite element model, and eigensolution is performed on the mass and stiffness matrices. The equation of motion for a multiple degree of freedom system is written in matrix form as:

$$[M]\{\ddot{x}\} + [C]\{\dot{x}\} + [K]\{x\} = \{F(t)\} \qquad (2.1)$$

where [M] is the mass matrix, [C] is the damping matrix, [K] is the stiffness matrix, {F(t)} is the forcing vector and {x} is the vector of displacements.

The so-called normal mode eigensolution is obtained using only the mass and stiffness matrix and assumes that the damping is either zero or proportional.

$$[[K] - \lambda[M]]\{x\} = 0 \qquad (2.2)$$

The eigensolution provides eigenvalues (frequencies) and eigenvectors (mode shapes).

2.2 Experimental Modal Model

The formulation of an experimental modal model is well documented and need not be developed for this purpose. The general equation for the frequency response matrix in terms of modal parameters is defined as:

$$[H(j\omega)] = \sum_{k=1}^{m}\left[\frac{\{U_k\}\cdot\{L_k\}}{(j\omega-\lambda_k)} + \frac{\{U_k\}^*\cdot\{L_k\}^*}{(j\omega-\lambda_k)}\right] - \frac{[LR]}{\omega^2} + [UR] \qquad (2.3)$$

Where:

$[H(j\omega)]$	=	Frequency Response Matrix
m	=	Number of modes in database
$\{U_k\}$	=	Mode shape vector for the kth mode
$[L_k]$	=	Row vector of modal participation factors
$[LR]$	=	Lower Residual Term
$[UR]$	=	Upper Residual Term
*	=	complex conjugate symbol
λ_k	=	Complex pole value for the kth mode, defined as:

$$\lambda_k = -(\xi_k\omega_{nk}) + j\omega_{nk}\sqrt{1-\xi^2{}_k} \qquad (2.4)$$

where ξ_k is the damping factor for mode k

and ω_{nk} = Natural Frequency of mode k

2.2.1 Least Squares Complex Exponential

A popular form of curve-fitting experimental modal data is the Least Squares Complex Exponential method. This method calculates the system poles in the time domain. The response can be expressed in terms of modal parameters in the time domain in the form of the least squares complex exponential:

$$[H(t)] = \sum_{k=1}^{m}\frac{1}{m_k\omega_{dk}}e^{-\lambda kt}\sin\omega_{dk}t \qquad (2.5)$$

Where:

ω_{dk}	=	Damped Natural Frequency of mode k
m_k	=	Modal mass of kth mode

2.2.2 Frequency Domain Mode Shape Estimation

Once the system poles are identified using the least squares complex exponential, the modal vectors are then estimated in the frequency domain using equation 2.3.

2.2.3 Mode Identification Tools

To aid in identifying poles in measured data, several tools exist for locating the number of modes in a given frequency band. Among the most common of these techniques are the FRF Summation, The Mode Indicator Function [3] and the Stabilization Diagram [4].

Enhanced Frequency Response Function

The simplest of mode indication tools is called the Enhanced Frequency Response Function or FRF Summation Function, and consists of a summation of all the measured frequency response functions. This will tend to accentuate modal peaks that exist in the data, which will appear as maxima in the summation of the imaginary components. However this technique is only effective when modes are reasonably well spaced in frequency, as closely spaced modes will appear as one in the summation.

Mode Indicator Function

The Mode Indicator Function is a tool available in many commercial software packages to aid in the identification of modes in measured data. The MIF is formulated to take advantage of the real component of the response vector being a minimum at resonance.

Stabilization Diagram

The stabilization diagram is tool used during the least squares complex exponential pole estimation process. The diagram identifies the stability of a pole as the order of the model is increased. Stability is defined for different modal parameters (frequency, damping and shape) as having less than some defined amount of change between successive order models.

2.3 Correlation techniques

Many tools are available for the evaluation of the correlation between FEA and test. A brief overview is given here and a more detailed treatment is contained in the references.

2.3.1 Modal Assurance Criteria (MAC)

The Modal Assurance Criteria is a commonly used method for assessing the degree of correlation between any two vectors and is formulated as

$$\{x_n\} = \begin{Bmatrix} x_a \\ x_d \end{Bmatrix} = [T]\{x_a\} \qquad (2.7)$$

where $\{a_i\}$ and $\{b_j\}$ are the vectors being compared.

3.0 Analysis

3.1 Analytical Model - Transfer Case Housings

The transfer case housings were modeled separately in MSC/NASTRAN using a combination of triangular and quadrilateral linear plate elements (CTRIA3, CQUAD4) and five and six sided (CPENTA, CHEXA) solid elements. The free-free normal modes from 0 to 1600 Hz were obtained via Lanczos eigenvalue extraction (SOL 103). The front case model consists of 8140 nodes and 7074 elements, and the rear cover contains 5062 nodes and 4668 elements. Figure 1 shows the finite element models of the housings.

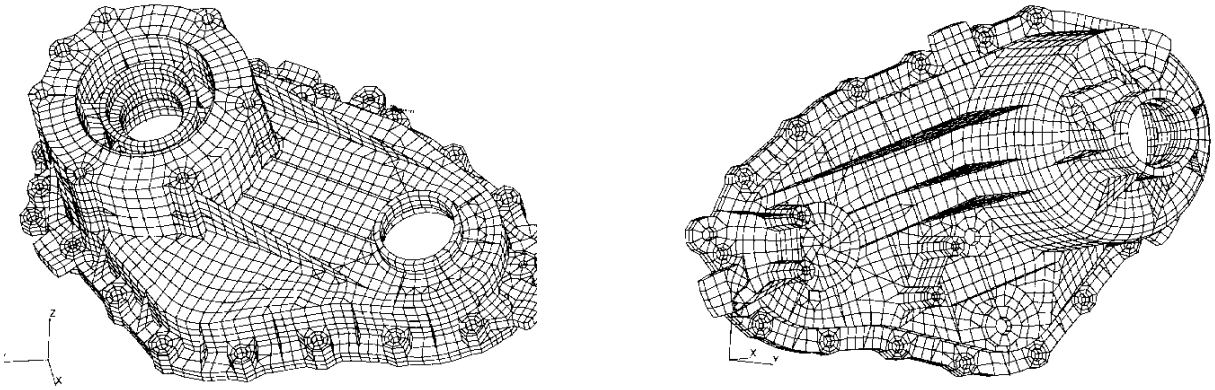

Case FEA Geometry *Cover FEA Geometry*

Figure 1

3.2 Experimental Model - Transfer Case Housings

The aluminum case and cover were tested to determine their modal parameters, modes shapes and natural frequencies. Each housing was tested individually. The experimental modal analysis (EMA) method was used. A matrix of frequency response functions was measured and the modal parameters were extracted using curve fitting techniques. All data acquisition and analysis was conducted using LMS CADA-X Software [5]

3.2.1 Test Configuration

A free-free test condition was desired to eliminate difficulties in modeling of the boundary conditions. This free-free condition was simulated using foam rubber supports. The supports provided suspension modes at less than one tenth the frequency of the first flexible modes (Figure 2 illustrates this) ensuring the boundary conditions of the test do not affect modal parameters.

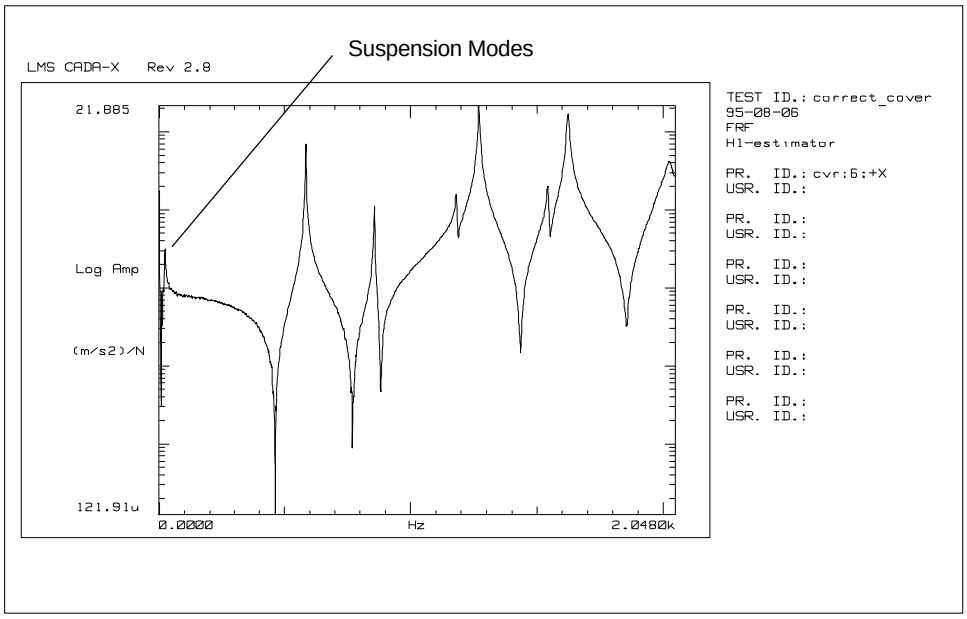

Figure 2 - Drive Point Frequency Response

Measurement locations were defined on the housings, and a wire frame geometry was created using 33 points on the case and 43 points on the cover. The geometry can be seen in Figure 3. The locations were chosen to give adequate spatial resolution to describe the global structural mode shapes.

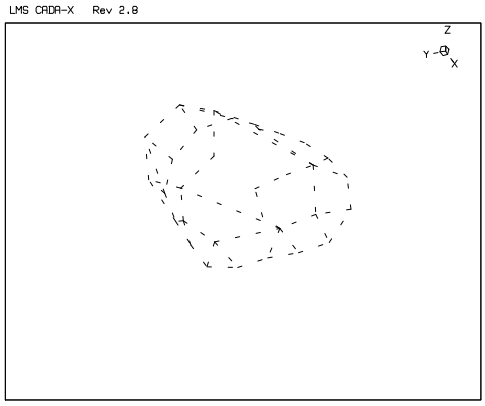

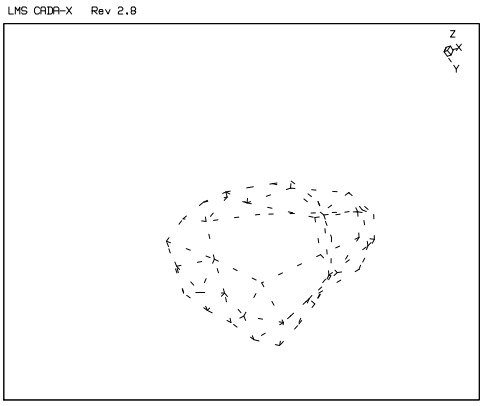

Case Measurement Geometry *Cover Measurement Geometry*

Figure 3

3.2.2 Frequency Response Measurements

Frequency Response Functions (FRF's) were measured at all of the measurement locations in three axes. Three methods can be used for this type of modal survey; fixed response (acceleration) with roving input (force), fixed input with roving response, or fixed input with response measured simultaneously at all locations. In each roving method, the roving measurement must be completed in three axes to adequately populate the FRF matrix. All three methods were used in this experiment. The force input was an impact hammer, the responses were measured with accelerometers.

The initial testing was done with a fixed input location (and direction), with accelerometers moved from point to point on the structure. The nature of the structure presented difficulty with this method, as the location of the accelerometer affected the dynamics of the structure significantly. This is referred to as "mass loading". The modal frequencies changed values depending on the location of the accelerometers making this method unacceptable. Figure 4 shows the modal frequencies shifting by up to 28 Hz due to accelerometer mass loading.

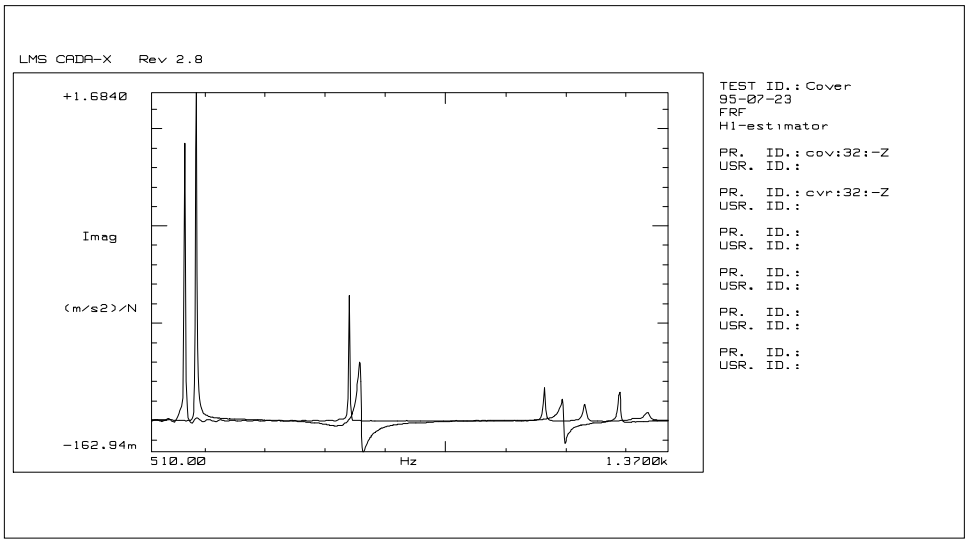

Figure 4 - Frequency Peak Shifting

The next test was attempted with accelerometer masses distributed at all of the measurement locations in attempt to reduce the frequency shifting. This method allowed many simultaneous response measurements. This also presented difficulties as the connection of all the masses decreased the modal frequencies, and introduced additional damping to the structure. The weights also caused additional local modes to appear in the structure, making it difficult to extract the global modal parameters. Figure 5 shows an FRF from this test.

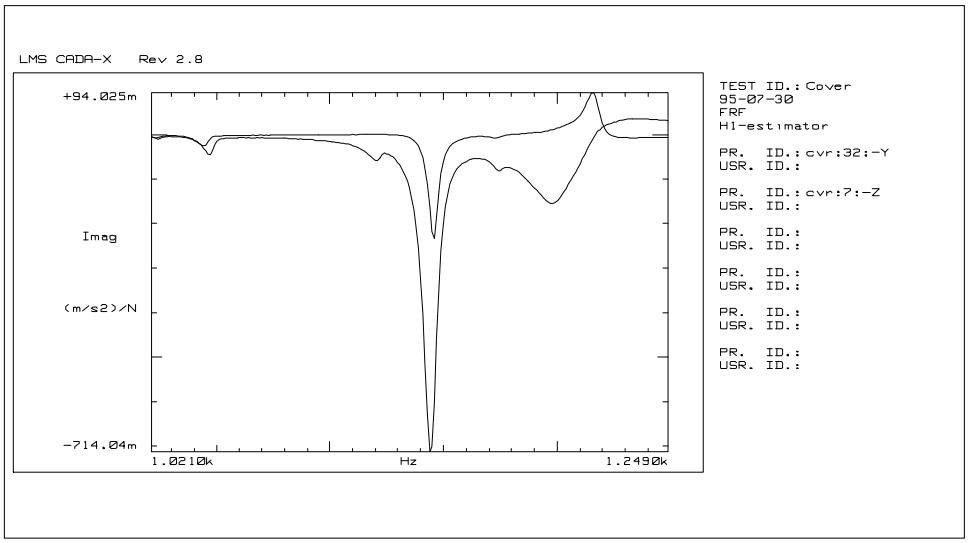

Figure 5 - Frequency Response With Multiple Accelerometers

The final test was to connect the accelerometer to a reference point, and excite the structure at all other points with the modal impact hammer. This method provided the best results with negligible mass loading. This was the most cumbersome method however, as the force input was required in three directions at all of the measurement locations. This required additional fixtures be attached to the structure so the force could be applied in three directions.

The FRF's were measured from 0 - 2048 Hz with a frequency resolution of 1 Hz. The hammer tip was chosen to provide a broadband excitation in this frequency range. The autopower spectrum of the excitation is provided in Figure 6. It can be seen from this figure that the input force rolls off at approximately 1600 Hz. This indicates that modes above 1600 Hz could not be properly excited.

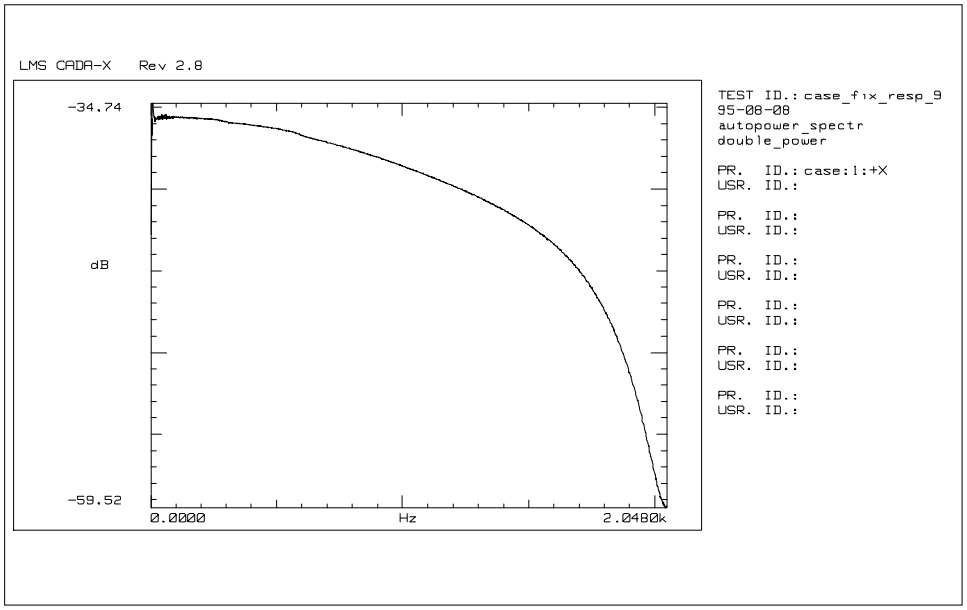

Figure 6 - Input Force Autopower Spectrum

The FRF's were collected for all measurement locations using a triaxial reference accelerometer at a location chosen both from visual inspection of the finite element mode shapes, as well as from a survey of drive point frequency responses from different points around the structures. Having a triaxial accelerometer as a reference provided three columns of the frequency response function matrix.

3.2.3 Modal Parameter Estimation

The poles (natural frequency and damping) and mode shapes were estimated using the polyreference modal parameter estimation (also known as the Least Squares Complex Exponential algorithm for poles, and the Frequency Domain for the mode shapes) . With the aid of the Mode Indicator Function (MIF) , Enhanced FRF and the Stabilization Diagram, the poles are selected. Figure 7 demonstrates the MIF and Sum Blocks. The mode shapes are then estimated using a least squares curve fitter.

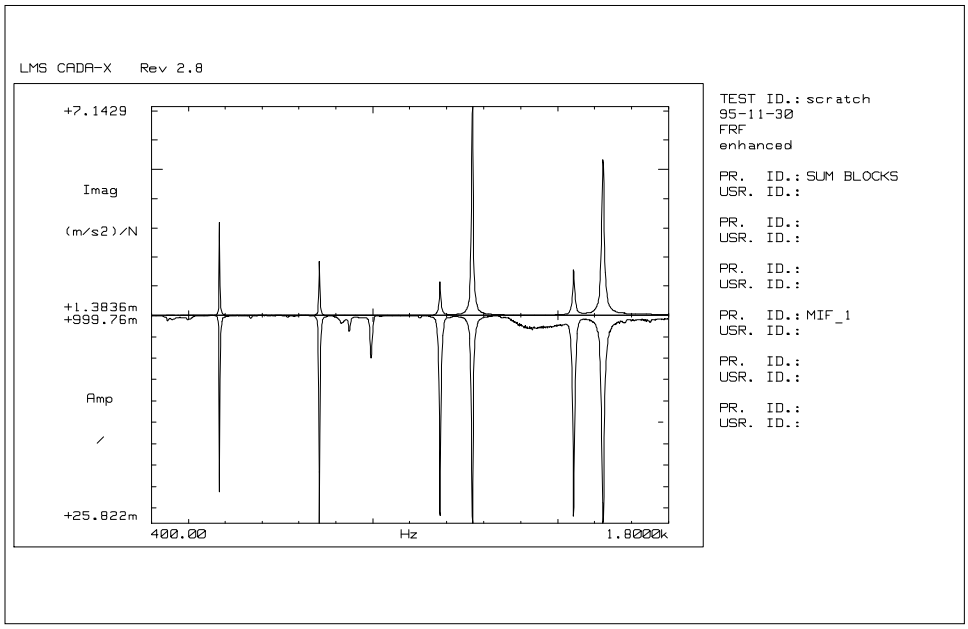

Figure 7 - Mode Indicator Function and Sum Blocks

4.0 Results

Since the test was configured to measure frequency response up to 1600 Hz, the finite element analysis was also conducted to calculate modes in that bandwidth. When the finite element analysis and experimental modal analysis were complete for both components, the first step in the correlation exercise was the comparison of the frequencies and shapes obtained.

4.1 Front Case Modes

Table 1 shows a list of flexible free-free modes of the front case below 1600 Hz extracted from the both the finite model and experiment.

Case FEA Frequencies	Case EMA Frequencies	Shape Description
607.36	646.9	Lateral Torsion
771.63	846.9	"Breathing" or Flexing of Open End
1151.57	1245.6	"Breathing" or Flexing of Open End
1317.49	1439	Vertical Bending
1553.63		Lateral Torsion

Table 1 - Front Case Modes

4.2 Rear Cover Modes

Table 2 shows a list of flexible free-free modes of the rear cover below 1600 Hz extracted from the finite element model and from experiment.

Cover FEA Frequencies	Cover EMA Frequencies	Shape Description
513.98	538.27	Plate Torsion
854.99	855.88	Plate and Extension Torsion
1104.20	1182.5	Plate First Bending
1156.37	1268.7	"Breathing" or Flexing of Open End
1397.76	1543.2	Plate Second Bending
1529.38		Plate Second Torsion

Table 2 - Rear Cover Modes

Note that in both the case and cover, one more mode was extracted from the FEA model in the 0-1600 Hz bandwidth. This, along with lower frequencies for the correlated modes, indicates the finite element models are more compliant than the actual parts as cast.

4.3 Correlation Analysis

To evaluate the correlation between the two databases, LMS LINK [6] correlation software was used to merge the LMS CADA-X data with the MSC/NASTRAN model information, via Neutral File transfer [7].

4.3.1 Weight Comparison

One simple way to compare a finite element model to the actual part is to compare the mass of the part to that of the sum of the elements in the model. This provides a first glimpse at how closely the finite element model represents the physical component, and is particularly important for dynamic analysis, where the mass distribution is a key contributor to the analysis results. Table 3 contains a comparison of the masses of the finite element models, calculated using published values for aluminum density, to those of the prototype transfer case housings.

	Prototype Parts (kg)	FEA Model (kg)	% Difference
Front Case	4.89	4.26	-12.9%
Rear Cover	3.95	3.52	-10.9%

Table 3 - Weight Comparison

This information reveals the finite element representations to be somewhat lighter than the actual parts. This is usually the case with die cast parts which tend to contain blend radii and fillets that are generally not represented in the model, in an effort to minimize geometric complexity.

4.3.2 Front Case Vector Correlation

For the front case component, four flexible modes under 1600 Hz were correlated. A visual inspection of the animated shapes indicated a reasonably good correlation. One discrepancy noticed for all four shapes was that the FEA modes have higher response levels at the sealing flange (open end) than the test vectors indicate. This suggests that the stiffness of this area may not be properly represented in the FEA model. Another significant discrepancy was noticed in the third mode shape, the appearance of a point of abnormally high response in the test vector at the lower face of the case. This may be due to a bad measurement. Figure 8 shows overlay plots of the first four experimental and analytical mode shapes.

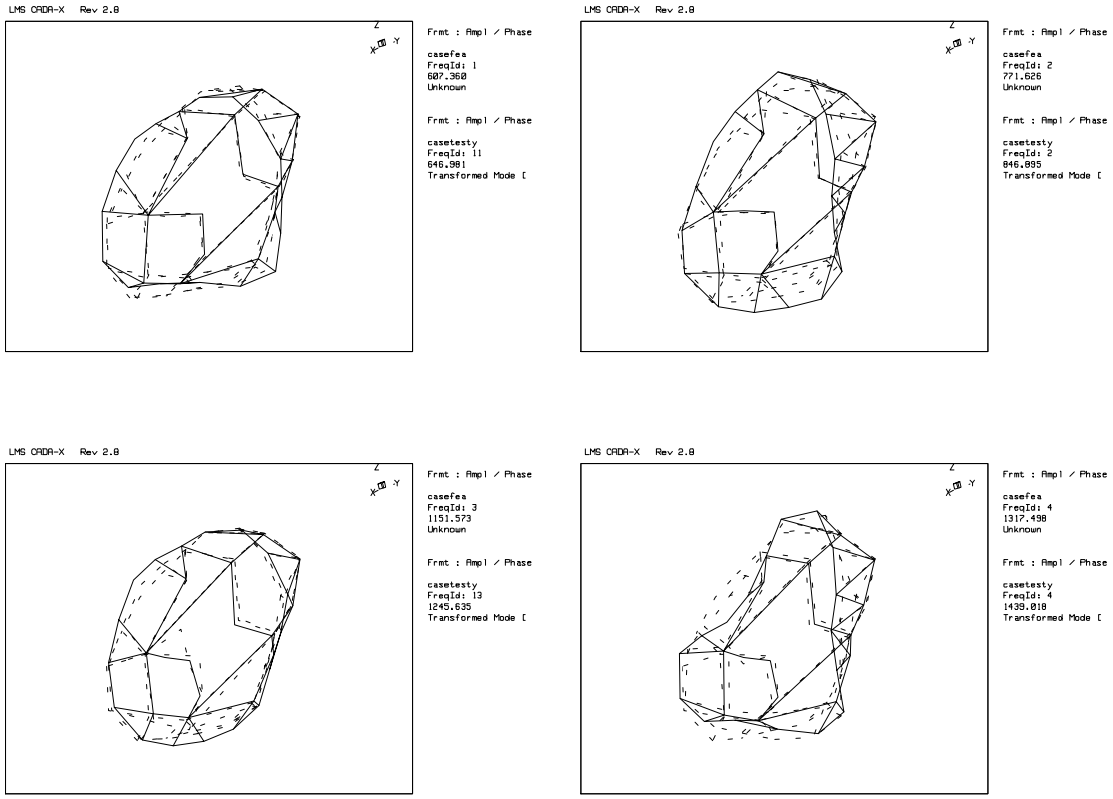

Figure 8 - Overlay of Analytical and Experimental Front Case Mode Shapes

The Modal Assurance Criteria (MAC) matrix is shown in Table 4. Despite good visual agreement between the animated shapes, the diagonal terms of the MAC do not indicate very good correlation, particularly for the third and fourth modes. The especially poor MAC value for the third mode may have been caused by the bad measurement point previously described.

	Test Frequencies			
FEA Frequencies	646.9	846.9	1245.6	1439
607.4	**0.7184**	0.0266	0.0001	0.0076
771.6	0.0227	**0.739**	0.0005	0.0001
1151.6	0.0028	0.0006	**0.3816**	0.0368
1317.5	0.0048	0.0012	0.0027	**0.5658**

Table 4 - MAC Matrix for the Front Case Model

4.3.3 Rear Cover Vector Correlation

As with the front case component, visual inspection of the rear cover animated shapes also suggested good correlation. Also like the case, the FEA model seems to have more compliance than the experimental model, particularly at the interface where the two components are joined in the assembly (sealing flange). One other major discrepancy occurred in all five correlated modes in one particular area. At the lower side of the rear face there are four tall bosses which are used to mount an external component to the back of the transfer case. The test model had a much higher level of response at measurement locations near these bosses than the FEA model. This discrepancy may be the result of some effect of instrumentation at this area, or some modeling error in this area of the structure. Figure 9 shows the first four experimental and analytical mode shapes of the cover overlaid.

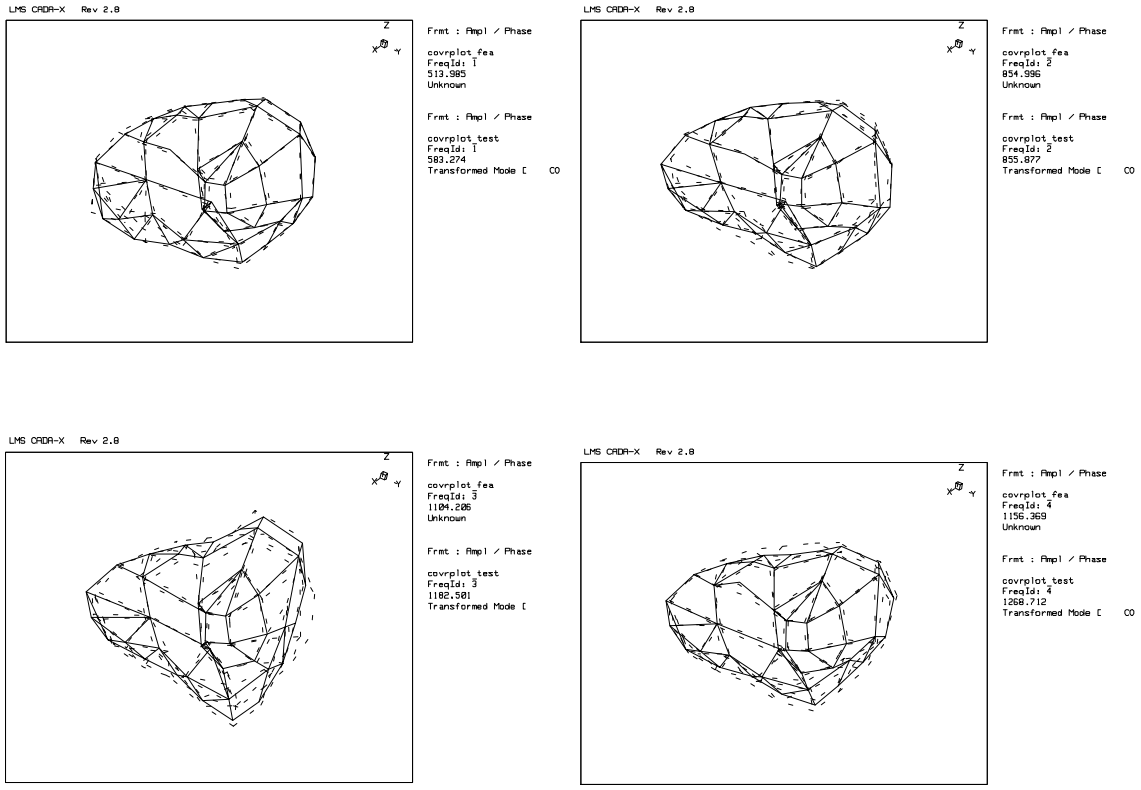

Figure 9 - Overlay of Analytical and Experimental Rear Cover Mode Shapes

The MAC values for the five correlated rear cover modes, while better overall than those of the front case, still would not generally be considered good. Again one reason for this may be the differences in compliance between the two databases, as well as the discrepancy at the mounting bosses. One other interesting trend is that the values steadily decrease with increasing frequency. This may be an indication that the quality of either or both of the models degrades at higher frequency.

	Test				
FEA	Frequencies				
Frequencies	583.27	855.88	1182.5	1268.7	1543.2
513.98	**0.76796**	0.01532	0.00179	0.04108	0.00492
854.99	0.00494	**0.74136**	0.01282	0.00189	0.00093
1104.20	0.00108	0.07592	**0.67407**	0.00063	0.00032
1156.4	0.03894	0.02894	0.00789	**0.64253**	0.00298
1397.8	0.00970	0.00027	0.00928	0.00951	**0.61108**

Table 5 - MAC Matrix for the Rear Cover Model

5.0 Discussion

Many problems were encountered during the testing, particularly with reference to mass loading, as discussed previously. Although these structures are relatively heavy relative to the mass of the accelerometer, mass loading was still significant, especially for modes with high participation from local areas with thin sections, such as ribs and plates. While these difficulties were overcome by changing to the roving impact measurement method, these measurement difficulties make this project a good candidate for the evaluation of non-contact measurement techniques.

The finite element model should be modified with lumped masses to simulate the reference accelerometers and some other instrumentation fixtures attached to the housings. There also appears to be some general modeling errors with regard to the stiffness distributions. For both components, the finite element model was more compliant at the sealing flange than the experimental model.

Large discrepancies in mode shape exist in the rear cover at the bosses. This is probably indicative of some modeling error at the interface between the plate and solid elements, and may be an opportunity for some local model updating study. The method of modeling the transition from solid to plate may require further study. A model updating procedure may also help reduce the global stiffness discrepancies, particularly at the sealing flange area of the housings.

6.0 Acknowledgments

The authors gratefully acknowledge the contribution of Kristine Maisonville and Chad Fair, both students of Michigan Technological University. Kris and Chad conducted much of the experimental work used in this correlation study. We would also like to acknowledge the contribution of Lohitsa, Inc., for their assistance in the development of the finite element models.

7.0 References

1) MSC/NASTRAN, Version 68.2, Finite Element Software from The MacNeal-Schwendler Corporation, Los Angeles, CA, 1995

2) Allemang, R.J., Brown, D.L., "A Correlation Coefficient for Modal Vector Analysis", Proceedings of the First International Modal Analysis Conference, 1982

3) Williams, R., Crowley, J.R., Vold, H. "The Multivariate Mode Indicator Function in Modal Analysis" Proceedings of the Fourth International Modal Analysis Conference, 1985

4) Crowley, J.R., Hunt, D. L., Rocklin, G.T., Vold, H. "The Practical Use of Polyreference Modal Parameter Estimation Method" Proceedings of the Third International Modal Analysis Conference, 1984

5) LMS CADA_X - Dynamic Test and Analysis Software, Version 2.8, Leuven Measurement Systems, Leuven, Belgium

6) LMS LINK - Dynamic Correlation, Sensitivity and Updating Software, Version 2.8, Leuven Measurement Systems, Leuven, Belgium

7) MSCNF - MSC/NATRAN to CADA_X Translation Utility, Version 2.7, O. Storrer, Leuven Measurement Systems, Leuven, Belgium, 1991